70(8A): 1-479; 2022. DOI: 10.18311/jmmf/2022/32044

Print ISSN : 0022-2755

Journal of Mines, Metals and Fuels

Contents available at: www.informaticsjournals.com/index.php/jmmf

Force Sensitive Resistors: A New and Emerging Field of Research in Conducting Polymers

Bhargav S[1], J Sundara Rajan[2]

[1]*Independent Researcher, Medical Electronics, Bengaluru 560070, email: bhargavrajan94@gmail.com, Mobile: 919945640408*
[2]*Electrical and Electronics Engineering, Siddaganga Institute of Technology, Tumkuru, E-mail: drjsrrajan12@ieee.org*

Abstract

Conducting polymers are fast evolving as a critical domain of research for industrial applications. With the advent of carbon conducting fillers, very high electrical conductivity of polymers is achieved. The polymers are biocompatible and are used for drug delivery, wearables and as sensors for industrial and medical electronics. Though the electrical conduction mechanisms are well correlated to the geometry, weight percentage and intrinsic properties of the conducting fillers, achieving a proper balance of electrical, mechanical and thermal properties has been a challenging task. This paper discusses the importance of conducting polymers in the development of force sensitive resistors which are extensively useful in industrial and medical applications. A brief review of conducting polymer matrices, conducting fillers and their properties which are critical for force sensing are discussed. Some of the important characteristic features of force sensing resistors are enumerated and few medical applications are presented.

Keywords: *Conducting polymers, force sensitive resistors, carbon fillers, electrical percolation, force sensor, quantum tunnelling.*

1.0 Introduction

Conducting polymers are at the forefront of polymer research and they represent a massive area of critical knowledge which is essential for developing future electrical and electronic devices. Recent advances in carbon nanofillers like carbon nanotubes and graphene have helped to achieve outstanding electrical conductivity coupled with good mechanical strength and thermal conductivity. Polymers with hybrid carbon fillers have been widely investigated for their utility in industrial applications and medical electronics. Conjugated polymers have shown tremendous improvement in both electrical and thermal conductivity, and hence application of polymers with carbon nanofillers have shown spectacular rise in recent years. Conductive polymers like polyaniline (PANI), polypyrrole (PPy) and poly (3,4-ethylenedioxythiophene) (PEDOT), have exhibited desirable properties for design of devices for emerging applications in electrical and electronics engineering. PANI is used in a wide range of applications including energy storage, biosensing with certain modifications, different types of sensors and supercapacitors. The physical characteristics of PANI are altered to meet the challenges of the end applications. It can be either in powder form, fiber or in the form of colloidal dispersion [1-2].

Polypyrrole (PPy), though identified during 1960 and reported during the years 1968-73 as a potential conductive material, it was only recognized in the year 1979 [3]. Extensive investigations have proved the utility of PPy in terms of simple fabrication techniques, stability in air and its capability for higher electrical conductivity [4]. PPy is used presently in many applications including solar cells, biomedical applications, energy storage, and more importantly in in electronic devices and sensors [5-6]. The physical attributes offer flexibility for variations, depending up on the route followed for synthesis and hence different forms such as films, nanospheres, and nanowires of PPy are available [7].

PEDOT emerged much later than PPy and PANI, though polythiophenes were well known in 1960. The conductivity of oligothiophene rings was studied during 1982 [8]. Many attempts were made to alter the structure of thiophene with side groups in order to improve its stability at par with those of PANI or PPy [9]. In the year 1988, the pioneering work of Bayer® of Germany highlighted the importance of dioxolane ring as key for improving its properties [10]. Since it is not easy to synthesise PEDOT, it is coupled with an anionic polymeric chain poly (styrene sulfonate) (PSS). Today, PEDOT:PSS is abundantly available on commercial scale. It is used in solar cells, organic transistors, OLED, bioelectronic devices, and sensors. It has comparable stability in air as compared to PANI and PPy, reasonable resistance to temperature and good mechanical properties, in addition to being very economical when processed on large scale.

Different allotropic forms of carbon are available in nature. Carbon is available with different structures and the main reason for growing popularity of carbon is its ability to form lattice with sp2 and sp3 hybrid orbitals. Graphite is widely used, and has sp2 hybridization with planar structure. The carbon allotropes generally possess lateral dimensions in the range of 1–100 nm and are termed carbon nanofillers. The evolution of carbon nanofillers coincided with the advancement of nanotechnology. Recent advances in polymer composites and the range of properties achieved is attributed to the broad range of properties of the carbon nanomaterials. Further advances with hybrid carbon fillers consisting of carbon nanotubes (CNT), graphene nanoplatelets (GNP) and carbon dots (CD) have resulted in spurt in opportunities for development of newer polymer composites with some unique characteristics.

Carbon dots are identified as a unique group of carbon which is endowed with distinctive optical characteristics which are comparable to conventional semiconductor quantum dots (QD) [11]. Since CD exhibit much higher biocompatibility and reduced toxicity than inorganic dots, they have emerged as a viable green alternative material for many bio-applications. Incorporation of CD in polymers have paved way for widening the scope of application of polymers, since many flexible properties are achieved. CD has also evolved as an indispensable tool for transforming polymers.

Conductive Polymers are manufactured by incorporation of carbon fillers using different dispersing methods into an insulating polymer matrix. The insulating polymers are benefitted by the conducting fillers and hence the composites exhibit high orders of electrical resistance. The semiconducting conducting polymer properties are tailored to exploit their properties for fabrication of tangible pressure sensors.

Rubbers, elastomer, and PDMS (Polydimethylsiloxane) are preferred polymer matrix, and the conducting phase consists of metal particles like nickel, copper, silver etc. In recent years carbon nanofillers are widely used for imparting higher electrical conductivity to the polymer matrix. The nanoparticle filler particles are in the range of few nm to tens of nm or mm in some cases. Such conducting polymers exhibit piezoresistive nature and are exploited for many sensors applications [12]. Typical applications are the light force/pressure sensors. The application areas consists of robotic manipulations, bio-medical applications, gate analysis in patients with Parkinson's disease (PD) and Human Machine Interfaces (HMI) [13]. The major drawback of these sensors is their poor repeatability and variations in accuracy over a period of time.

2.0 Electrical Conduction

Electrical conduction in conducting polymers is by tunnelling mechanism across the conducting filler particles in the polymer matrix. In Fig.1, a schematic illustration of the conducting polymer is depicted. There are two metal electrodes with the polymer matrix sandwiched between them. Some conducting fillers are in contact with the metal electrodes, and some are randomly distributed within the epoxy matrix. The resistance of the force sensitive resistor consists of two components, one due to the contact resistance between the conducting filler and the metal electrodes and the other due to the bulk of the polymer with distributed filler particles. Considering a simple case, for ease of discussion, the overall resistance of the FSR can be represented by the equation:

$$R_{FSR} = R_{bulk} + 2R_C \quad \text{... (1)}$$

In this equation, R_{bulk} represents the overall resistance of the polymer due to tunnelling mechanism and R_C is the contact resistance between the metal electrodes and the conducting fillers. Since two electrodes are involved, factor $2R_C$ is considered. The series connection between Rbulk and $2R_C$ with application of strain σ constitutes the *FSR* as shown schematically in Fig.1, when the FSR is acted upon by an external stress (s) and therefore the inter-filler particle distances are reduced. For the same reasons, the inter-particle separation which constitutes the tunnelling bridges is also lowered. In order to overcome complications arising due to the two different mechanisms, and to bring in clarity, the basic differences between the conducting polymer and the FSR would be mandatory. Some authors have proposed a model [14], decomposing the resistance of the FSR (R_{FSR}) into two components as shown in equation:

$$R_{FRS} + R_{Bulk} - 2R_C \quad \text{... (2)}$$

In this equation R_{Bulk} is the resistance of the conducting polymer which has its origin from the tunnelling mechanism of electrical conduction, R_C is the contact resistance between the metal electrodes and the conductive filler. The combination of R_{Bulk} and $2R_C$ constitutes the resistance of FSR.

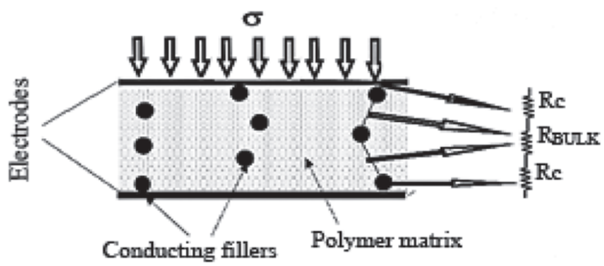

Figure 1: Schematic depicting the polymer matrix with conducting fillers in an FSR being subjected to stress (s) and the formation of series, contact and bulk resistance

In terms of potential drop across the FSR, due to tunneling, the following equation can be used to represent the components of VFSR, the potential that develops across the resistance of FSR:

$$V_{FSR} = 2V_{RC} + V_{Bulk} \quad \text{... (3)}$$

In this equation VRC is the potential drop across the contact resistance and VBulk is the potential drop across the tunnelling resistance RBulk. The corresponding electrical circuit representation is shown in Figure 2a and 2b. For simplicity, the tunneling barrier is assumed to be rectangular with a barrier height Va and width σ as shown in Figure 2c. The barrier width σ is a direct measure of the inter filler particle distances.

From the physics of conducting polymers, it is known that at the percolation threshold, that two modes of electrical conduction namely ohmic conduction and tunnelling conduction takes place. The flow of current at electrical percolation is across the interconnecting fillers in a polymer matrix and it is ascribed by two distinctive parameters namely the intrinsic resistance of the conducting fillers which are in direct contact or in close proximity and the other due the insulating layers between the fillers. Therefore, across the percolation path, the contact resistance ($R_{Contact}$) is specified as the sum of the contact resistance of fillers (R_C) in the absence of insulating layer and the tunneling resistance (R_t) in presence of the insulating layers between the fillers. Therefore, RContact is given by the equation:

$$R_{Contact} = R_C + R_t \quad \text{... (4)}$$

Further RC and Rt show dependance on the parameters of the conducting polymer which is expressed by the following two equations:

$$R_C = \frac{1}{\sigma_f}\frac{1}{2d\varphi} \quad \text{... (5)}$$

$$\sigma_{dc} = \frac{\pi}{16d}\frac{1}{R_{Contact}} \quad \text{... (6)}$$

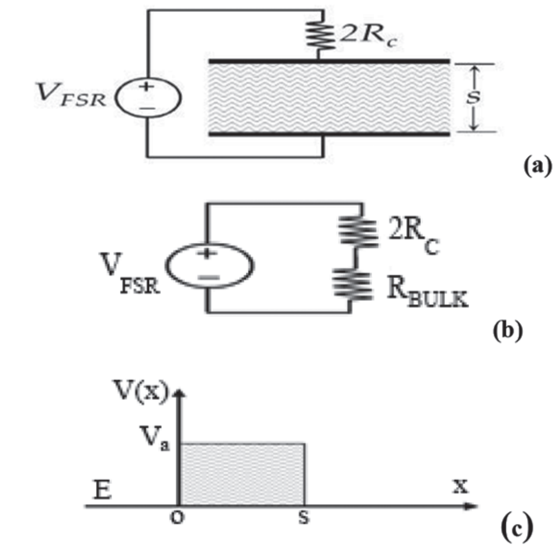

Figure 2: (a) Electrical circuit representation of FSR, (b) series combination of contact resistance (RC) and tunnelling resistance (RBulk) and (3) Quantum rectangular barrier (height Va and width s) for a particle of electron energy E

Here σ_f represents the intrinsic DC conductivity of filler, which is extremely high for carbon fillers, d is the dimension of the filler. Typically, it is the diameter in case of MWCNT or thickness in case of graphene nanoplatelets and φ is the volume fraction of the filler. The tunnelling resistance in case of conducting polymers is computed based on the relation:

$$R_t = R_{Contact} - R_C \quad \text{... (7)}$$

From equation 5, it is observed that RC varies inversely with DC conductivity of the conducting filler, the volume fraction φ of the filler, and its diameter or thickness d. The contact resistance R_C of the fillers is minimised by using fillers of very high electrical conductivity, or with fillers of larger dimensions or alternatively by using higher volume fraction of the filler. The electrical conductivity of GNP is three to four orders higher than that of carbon nanotubes, and the value of d is around 7nm for GNP and 16nm in case of MWCNT. Thus GNP has a dominant role on the effective contact resistance. It is also known that for a given volume fraction of the conducting filler, RC of MWCNT will be 400 to 450 times the value of GNP. The dominance of GNP in reducing R_C is well recognized. Therefore it is always advantageous to use GNP for developing conducting polymers for FSR.

In a practical FSR, the contact resistance depends on the plastic and elastic interactions that occur between the conducting filler particles and the inner surface of the electrode. The contact resistance depends on the filler particle diameter, the nature of interactions taking place at the interfaces and the stress which is normally applied along the surface of the electrode. The dependence of the contact resistance on the applied pressure is observed to follow a power law dependence [15]. When a large mechanical stress (σ) is applied, the contact resistance is stated to decrease based on the relation $R_c \propto \sigma^{-1/3}$ for elastic reactions or it follows the relation $Rc \propto \sigma^{-1}$ for plastic interactions. However, some authors [14] have expressed their disagreement for either the $\sigma^{-1/3}$ or σ^{-1} dependence of R_C due to difficulties in experimental validation of these parameters.

When FSR is subjected to incremental stress, three mechanisms come into play. These include

(i) the contact resistance of the existing conducting paths, which is lowered based on power laws dependence ($Rc \propto \sigma^{-1}$ or $R_c \propto \sigma^{-1/3}$),

(ii) newer contact paths that may be formed to reduce the contact resistance further and

(iii) the average inter-particle distances which are lowered and the consequent reduction in the tunnelling resistance (R_{Bulk}). The second mechanism tends to increase the area for tunneling conduction (A). The overall effect of the first and second mechanisms based on power law dependence for modelling the contact resistance is not accepted for its generality by many authors. Based on commercially available FSR, some authors [16] have proposed a modified relation for contact resistance RC, and it has the form:

$$R_C = R_{par} + \frac{R_C^0}{\sigma^\alpha} \quad \text{... (8)}$$

In this equation R_{par} is the total resistance of the conducting particles, R_C^O is the contact resistance when the applied stress does not exist, but the contribution arises from the offset stress originating from the encapsulation of the sensor. The factor σ^α accounts for variations in the applied stress, by introducing an exponent α. Since the polymer matrix bonds the components of the FSR around the edges, the conducting polymer is stated to be preloaded with an offset stress α_0. Thus, even when the FSR is not subjected to stress, there exists a finite value of the contact resistance. Since the offset stress is normally much lower than the applied stress (σ^α), ignoring σ_0 factor is valid in equation 8. When the input voltages across FSR is higher, contribution from the bulk resistance (R_{Bulk}) would be negligible as compared to R_C. Hence it is valid to approximate RFSR as being equal to R_C for higher values of V_{FSR}.

3.0 Response of FSR

The FSR response is accomplished by the measurement of potential that develops across resistance RFSR with a voltage divider consisting of typically a 10 kΩ resistor in series with the resistance of RFSR. The voltage drop across R_{FSR} changes in response to the applied stress. A typical voltage divider circuit is shown in Fig.5. For V_S of 5V (typical value used in microcontrollers), the applied stress produces a V_{FSR} which can fluctuate if the stress across FSR is high. In some cases V_{FSR} swings from a few millivolts up to 5V, leading to poor repeatability. It is also preferable to use buffered output with amplifiers in the inverting mode to overcome the problem. However, if the load bearing capability of the FSR is high, and the expected strain is much below the rated strain of the FSR, only small potentials would develop across the resistance of FSR and large fluctuations in potential is avoided. However, measurement of millivolt signals may be challenging in outdoor unshielded environments, because of the high ambient noise levels.

The electrical resistance developed across FSR due to mechanical deformation is quantitatively determined by using a gauge factor (GF) which is given by the equation [17]:

$$GF = \frac{\Delta R\, R_0}{\sigma} \quad \text{... (9)}$$

In this equation, R_0 is the initial resistance and ΔR is the difference in resistance when strain is σ is applied. The piezoresistive sensitivity of the

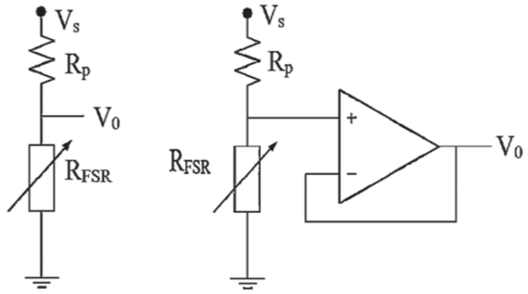

Figure 3: Voltage divider for FSR with unbuffered and buffered output [15].

conducting polymer has contributions from the intrinsic and the geometrical piezoresistive effects [17]. The piezoresistive bending response with GF≈1 shows stability of the FSR even when the FSR is subjected to strain cycling up to temperatures of 40°C.

3.1 FSR parameters

FSR is expected to respond to external stimuli selectively (different magnitudes of strain, at different temperatures and humidity) with good sensitivity and linear response. Strain sensors mandatorily should respond systematically to stimuli, such as tensile and compression, without any change in their characteristics. The performance of strain sensors is evaluated in terms of its sensitivity, operational range, response and recovery time, stability, and repeatability [18]. Some of these parameters are defined as follows:

i. **Sensitivity:** The least measurable variations in electrical signals in response to the applied strain is termed the sensitivity. The strain sensors response is recorded as an electrical output and, even as optical measurements. The sensitivity is based on determination of the gauge factor (GF).

ii. **Operational range:** A liner response of strain sensor over a wide working range of strain helps the user to select appropriate FSR for any given application. The response may be in terms of voltage, current or the output of the FSR.

iii. **Response time:** The time within which the sensor starts responding by way of electrical signal (resistance R) or it is an optical response which is a reaction to the applied strain which is imposed (Δt_1 as shown in Figure 6a.) is a measure of the response time. Lower the response time, better would be the performance of the sensor.

iv. **Recovery time:** The time period in which the sensor returns to its original state in terms of resistance (resistance R_0) after relaxation or removal of strain is referred to as the recovery time (shown as Δt_2 in Figure 6a). A sensor should invariably possess an incredibly low response and recovery time for applications in cardiac monitoring like heart beats, human brain signals, wearable e-skins and other medical applications.

v. **Stability:** The stability of the strain sensors is a serious challenge to the application of wearable sensors in real-time applications and it has obstructed rapid developments in IoT applications. Analysis of rapid human muscle movements and determination of blood flow volumes has dictated the need for more stable recovery of strain-sensing devices.

vi. **Hysteresis (H):** It is a measure of the response of the sensor to the initial stimulus and the difference between successive strain cycles. For a stable operation of the strain sensors, the electrical hysteresis is expected to be minimal (ΔH_1, ΔH_2 of Fig.6b). It implies that when the strain sensor is taken through a cycle of identical strain with time intervals in between, the difference in response to the strain at each level should be extremely low. Other parameters like electrical response lifetime and storage stability are not very critical in industrial applications since the number of operations and storage conditions and durations are always specified for optimum operation of the device.

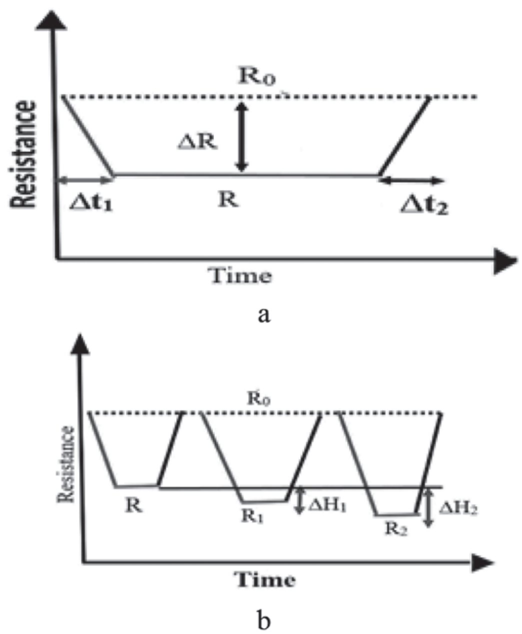

Figure 4: Typical response of FSR (a) strain response and recovery time, (b) hysteresis

4.0 Medical applications

(A). Application in cardiology

Some authors [19] have used non-invasive analysis of coronary vascular diseases (CVD) for real-time monitoring of arterial wave-pulse characteristics using parameters like heart rate, reflectivity index, pulse wave velocity and others. The FSR is strategically placed on the carotid or radial artery of the patient. The differences resulting in the volume of blood flow through the arteries which is caused by the variations in the systolic and diastolic phases of the cardiac cycle, tend to exert force on the FSR, leading to the generation of corresponding bio-signals. The bio-signals are acquired and converted to digital signals for determination of the critical parameters of the heart. The authors have used circular FSR (FSR402) which is placed on the radial artery. The deployment of FSR makes it easier for the recording of the arterial wave pulses. In order to estimate the accuracy of the measurement, conventional Photoplethysmopgraphy has been used and the and the reported accuracy is within ±3%.

(B) Diagnosis of Sleep Apnea

Some authors [20] have used FSR 406 sensor, having 38 mm of sensing area for diagnostics of sleep disorders. The FSR is placed over the thoracic or chest cavity region. Thoracic cavity has the rib cage on the sides and top, and the diaphragm at the bottom. The force experienced by the FSR is monitored through the changes in the resistance. At higher force, the resistance decreases and hence the voltage drop across the FSR increases. Typical respiratory rates in adults is between 16 and 20/minute and in infants it is 100/minute, and the corresponding maximum signal frequency is 2Hz. The authors have used a simple first order low pass filter with cut-off frequency 2Hz for signal conditioning. The circuit is cascaded with a Twin T notch filter to eliminate line noise frequency. By using a computer aided real-time sleep apnea monitoring system integrated with an FSR, an accuracy of 95% is reported.

(C) Cane for Parkinson's Disease (PD)

PD is a chronic disorder of the human brain. It affects the way the brain co-ordinates the motor functions of the human body. A part of the brain called the Substantia Nigra is mainly affected in patients suffering from PD. From literature, it is observed that many attempts are being made to rehabilitate PD patients with the application of modern technologies. The design of the cane for PD patients focuses on helping the patients in (i) detection of freezing of gait (FOG) and (ii) mitigation of FOG by recording vital data from sensors to analyze gait during the progression of PD. Freezing of gait (FOG) is a serious incapacitating clinical occurrence characterised by brief bouts of inability to walk or the tendency to take short steps which typically initiates gait. A cane handle with few FSR's fixed is shown in Fig. 7. It is used for detection of the force exerted by the patient in holding the handle. During the initiation of FOG, the force on the handle increases gradually and monitoring FSR output helps in the detection of the stability of the patient and the initiation of FOG.

Figure 5: Cane handle with FSR 1,2 and 3.

5. Conclusions

Developments in the domain of conducting polymers have led to expansion of innovative sensors which have wide ranging applications in the industry, medical diagnostics and IoT technology. This paper has reviewed the importance of conducting polymers and the role of different conducting fillers. The concept of electrical percolation can be explored further to develop better sensors. However, extensive studies on the effect of conducting filers at percolation in the resulting properties of FSR would be highly desirable.

The use of semiconducting polymers for development of force sensitive resistors is discussed and their properties which are crucial for a given application are explained in brief. Typical examples of FSR in few medical applications are highlighted to underline the importance of innovations in the technology of conducting polymers. There is need to further enhance the sensitivity, accuracy and repeatability of FSR, so that more application areas could be identified in the future.

6.0 References

[1] Ben, J.; Song, Z.; Liu, X.; Lu, W.; Li, X. Fabrication and Electrochemical Performance of PVA/CNT/PANI Flexible Films as Electrodes for Supercapacitors. *Nanoscale Res. Lett.* 2020, 15.

[2] Kazemi, F.; Naghib, S.M.; Zare, Y.; Rhee, K.Y. Biosensing Applications of Polyaniline (PANI)-Based Nanocomposites: A Review. *Polym. Rev.* 2020, 1–45..

[3] Diaz, A.F.; Kanazawa, K.K.; Gardini, G.P. Electrochemical polymerization of pyrrole. *J. Chem. Soc. Chem. Commun.* 1979, 635–636.

[5] Watanabe, A.; Tanaka, M.; Tanaka, J. Electrical and Optical Properties of a Stable Synthetic Metallic Polymer: Polypyrrole. *Bull. Chem. Soc. Jpn*. 1981, 54, 2278–2281.

[6] Biswas, S.; Drzal, L.T., Multi-layered nanoarchitecture of graphene nanosheets and polypyrrole nanowires for high performance, supercapacitor electrodes. *Chem. Mater.* 2010, 22, 5667–5671.

[7] Bao, L.; Yao, J.; Zhao, S.; Lu, Y.; Su, Y.; Chen, L.; Zhao, C.; Wu, F. Densely Packed 3D Corrugated Papery Electrodes as Polysulfide Reservoirs for Lithium-Sulfur Battery with Ultrahigh Volumetric Capacity. ACS Sustain. *Chem. Eng.* 2020, 8, 5648–5661.

[8] Tourillon, G.; Garnier, F. New electrochemically generated organic conducting polymers. J. Electroanal. Chem. Interfacial Electrochem., 1982, 135, 173–178.

[9] Guillerez, S.; Bidan, G. New convenient synthesis of highly regioregular poly(3-octylthiophene) based on the Suzuki coupling reaction. *Synth. Met.* 1998, 93, 123–126

[10] Heywang, G.; Jonas, F. Poly(alkylene dioxythiophene)s, New, very stable conducting polymers. *Adv. Mater*. 1992, 4, 116–118

[11] Lim, S.Y.; Shen, W.; Gao, Z. Carbon quantum dots and their applications. *Chem. Soc. Rev.* 2015, 44, 362–381. .

[12] Mei, H.; Zhang, C.; Wang, R.; Feng, J.; Zhang, T. Impedance characteristics of surface pressure-sensitivecarbon black/silicone rubber composites. Sens. Actuators A Phys. 2015, 233, 118–124.

[13] Verdejo, R.; Mills, N. Heel-shoe interactions and the durability of EVA foam running-shoe midsoles. *J. Biomech*. 2004, 37, 1379–1386.

[14] Leonel Paredes-Madrid, Arnaldo Matute, Jorge O. Bareño, Carlos A. Parra Vargas and Elkin I. Gutierrez Velásquez, "Underlying Physics of Conductive Polymer Composites and Force Sensing Resistors (FSRs).A Study on Creep Response and Dynamic Loading", *Materials* 2017, 10, 1334.

[15] Mikrajuddin, A.; Shi, F.; Kim, H.; Okuyama, K. Size-dependent electrical constriction resistance for contacts of arbitrary size: From Sharvin to Holm limits. Mater. Sci. Semicond. Proc. 1999, 2, 321–327.

[16] Paredes-Madrid, L.; Palacio, C.; Matute, A.; Parra Vargas, C. Underlying Physics of conductive Polymer Composites and Force Sensing Resistors (FSRs) under Static Loading Conditions. *Sensors* 2017, 17

[17] J. Teixeira, L. Horta-Romarís, M.-J. Abad, P. Costa, S. Lanceros-Méndez, Piezoresistive response of extruded polyaniline/(styrene- butadiene-styrene) polymer blends for force and deformation sensors, *Materials & Design*, Volume 141, 2018, Pages 1-8.

[18] Loganathan Veeramuthu, Manikandan Venkatesan, Jean-Sebastien Benas, Chia-Jung Cho, Chia-Chin Lee, Fu-Kong Lieu, Ja-Hon Lin, Rong-Ho Lee and Chi-Ching Kuo, Recent Progress in Conducting Polymer Composite/Nanofiber-Based Strain and Pressure Sensors, *Polymers* 2021, 13, 4281.

[19] Susmitha Wils K, George Mathew, M. Manivannan, Suresh R Devasahayam, A Comparison of Pinch Force between Finger and Palm Grasp techniques in Laparoscopic Grasping, Engineering, 2012, 5, 46-49 doi:10.4236/eng.2012.410B012 Published Online October 2012.

[20] Sundar A, Das C, Low cost, high precision system for diagnosis of central sleep apnoea disorder, Proceedings of 2015 International Conference on Industrial Instrumentation and Control (ICIC 2015), Pg.354-359.